

Evaluation of electrode-semiconductor barrier in transparent top-contact polymer field effect transistors

Manohar Rao and K. S. Narayan^{a)}

Jawaharlal Nehru Centre for Advanced Scientific Research, Jakkur, Bangalore 560 064, India

(Received 27 March 2008; accepted 9 May 2008; published online 5 June 2008)

Interfacial barriers at the metal-semiconductor junction manifest in the form of sizable contact resistance in polymer field effect transistors (PFETs). We study the barrier using optical excitation directed specifically beneath the electrodes in the top-contact PFETs without optically perturbing the channel. Differences in the transconductance responses with the light localized at the source and the drain electrode region provides a considerable insight into the injection barriers. © 2008 American Institute of Physics. [DOI: 10.1063/1.2938059]

The performance of thin film field effect transistors based on conjugated organic material as the active semiconducting component has improved over the years and holds great promise in large-area low cost applications.¹ The electrical characteristics of polymer field effect transistors (PFETs) shows deviation from ideal field effect transistor characteristics, due to factors such as contact resistance (CR),² gate voltage dependent mobility μ ,³ bias-stress instability,⁴ and time evolution of μ .⁵ The lower CR in top-contact PFET structure compared to bottom contact structure is attributed to a variety of reasons such as larger effective area of contact² and increased order of the film.⁶ A lower barrier is generally observed using photoemission measurements for metal films deposited on the organic semiconductor layer compared to organic semiconductor grown on metal substrate.⁷ The energy barrier limits the charge injection process into the organic semiconductor. The low μ polymer further lowers the injection efficiency due to the larger dwell period of the injected charge carrier near the contact prior to the bulk transport, which results in recombination with their image charge.⁸ The estimate of CR is typically obtained by studying the FET characteristics using the scaling-law method by fabricating a set FETs of varying channel length (L).⁹ Large statistical variations are commonly observed in the $R(L)$ plots for polymer FETs unlike the case of small molecule FETs or amorphous Si TFTs. $R(L)$ profile is less reliable in PFETs to arrive at an accurate estimate of CR. In this regard, a direct assessment for CR from the polymer device would be quite valuable. Some of these methods include transfer-line method,¹⁰ four-probe measurement,¹¹ and scanning probe potentiometry,¹² which allows for a separate determination of CR at source and drain electrodes from a single FET.

In this work, we introduce an approach to study the interfacial barrier by selective illumination of polymer at the electrode regions and study the variations of its transconductance responses. The method is particularly applicable for top-contact FETs where the substrate dielectric is transparent and electrodes are wide enough to have the excitation sufficiently far away from the channel region, thereby avoiding a direct contribution from the photogenerated carriers to the channel current. We carry out these studies for FETs based on poly(3-hexylthiophene) (P3HT) and methanofullerene [6,6]

Phenyl-C₆₁-butyric acid methyl ester (PCBM) blend. The possibility of larger quantum efficiency for carrier generation in P3HT-PCBM while maintaining μ provides a better platform to demonstrate the concept.

Regioregular P3HT was obtained from sigma aldrich and purified using reprecipitation method. Unpatterned indium tin oxide (ITO) sputtered glass slides was used as transparent gate electrode. Thin dielectric films of divinyltetramethyldisiloxane-bis(benzocyclobutene) (BCB) with thickness $\sim 1 \mu\text{m}$ was spin coated on the substrate and treated as per established procedures. P3HT films of typical thickness $\sim 100 \text{ nm}$ was spin coated on the treated dielectric film from 10 mg/ml chloroform solution and annealed as per standard procedures. Gold (Au) source-drain (S-D) contacts were thermally deposited using shadow mask, to fabricate devices with the following dimensions: channel length L of $\sim 40 \mu\text{m}$, channel width w of $\sim 2 \text{ mm}$, and electrode span $b \sim 5 \text{ mm}$. The optical beam size from a 633 nm He-Ne source incident from ITO side was much less than w and b for the measurements. The channel region between the S-D electrodes was suitably masked to avoid any collection of direct and scattered light. PFETs fabrication and electrical characterization were carried out in inert conditions.

The P3HT based FET characteristics [Fig. 1 (inset)] were similar to the earlier reported results of μ_{FET} , $I_{\text{on}}/I_{\text{off}}$ ratio, and threshold voltage V_{th} from our laboratory.^{13,14} The transfer curves did not exhibit any appreciable hysteresis for the range of sweep rates ($\sim 0.1 \text{ V/s}$) used. The μ_h in the saturation regime was obtained from $I_{\text{ds}}(V_g) = \{w/2L\} \mu C_i (V_g - V_{\text{th}})^2$ where C_i is the capacitance per unit area of the gate dielectric $\approx 2.3 \text{ nF/cm}^2$. The measured μ_h for the saturation regime and V_{th} obtained by plotting $\sqrt{I_{\text{ds}}}$ versus V_g for a large number of devices were in the range of $\approx (0.2-5) \times 10^{-3} \text{ cm}^2/\text{V s}$ and $0-7 \text{ V}$, respectively. The introduction of PCBM moieties in the P3HT matrix in case of the P3HT-PCBM blend FETs did not vary μ but a shifted V_{th} to higher positive voltages with $\mu_{\text{hole}} \approx 10^{-3} \text{ cm}^2/\text{V s}$ and $V_{\text{th}} \approx 15 \text{ V}$.

The measurements involving photoexcitation of the electrode region were carried out by ensuring dark conditions in the channel region. The dark current characteristics and the history of the device prior to illumination at the source and drain regions were identical. The changes introduced by the photoexcitation of channel region arise from a complete different set of photophysical processes leading to large varia-

^{a)}Electronic mail: narayan@jncastr.ac.in.

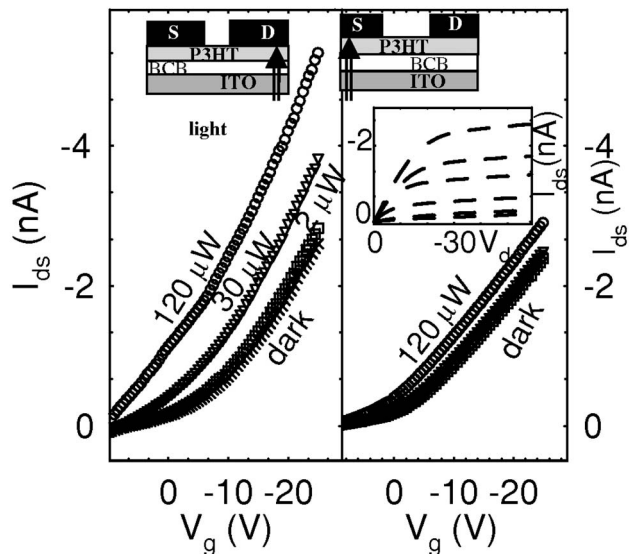


FIG. 1. Transfer characteristics of top-contact P3HT FET at $V_{ds} = -10$ V, with (left) light incident selectively on the drain electrode region as depicted in the schematic (not to scale) and (right) light incident selectively on the source electrode region. The inset is the dark I_{ds} - V_{ds} response for P3HT FET at different V_g (5 to -20 V in steps of 5 V).

tions in I_{ds} (by several orders) which is not the main theme of this paper and is discussed in detail elsewhere.^{13,14} The illumination volume in this case was confined to region beneath the source electrode and the drain electrode, which was at a sufficient and equal distance, of 3 mm away from the channel edge [Fig. 1 (inset)]. At $\lambda = 633$ nm (low absorption region) with light incident from the substrate side, the photoactivity is largely restricted at the P3HT-electrode interface region. The zone of activity at the interfacial region was ascertained by comparing the responses using $\lambda = 633$ nm and $\lambda = 532$ nm (where absorption is high) sources for films with different thicknesses and observing minimal changes in I_{ds} for the latter case.

At low incident power (< 1 nW), subtle changes in I_{ds} - V_g characteristics are observed, and at higher incident power (P), a clear trend in the $I_{ds}(P)$ and $V_{th}(P)$ is present. Figures 1(a) and 1(b) show the transconductance behavior of the PFET under selective illumination at the drain and source electrode regions. The transconductance characteristics for varying light intensity at both the electrodes region were measured for the linear and saturation regimes. The general trend of a larger $I_{ds}(P)$ and dI_{ds}/dP for illumination under the D region was observed and compared to the S region for both linear and saturation regime. The dI_{ds}/dP (at $V_g = -25$ V) showed a linear response and was in the range of 0.004 and 0.02 nA/ μ W for light incident at source and drain electrode, respectively.

The selective increase of I_{ds} upon photoexcitation on the drain electrode region compared to the source electrode region was observed only in the enhancement mode of operation and changes were not noticeable in the depletion mode. This observation is strikingly in contrast with the changes observed in PFETs when the entire channel is illuminated, and where a significant I^{light}/I^{dark} (up to 10^6) is observed in the depletion mode with the photoinduced current magnitude approaching values corresponding to the current in the enhancement mode.¹³

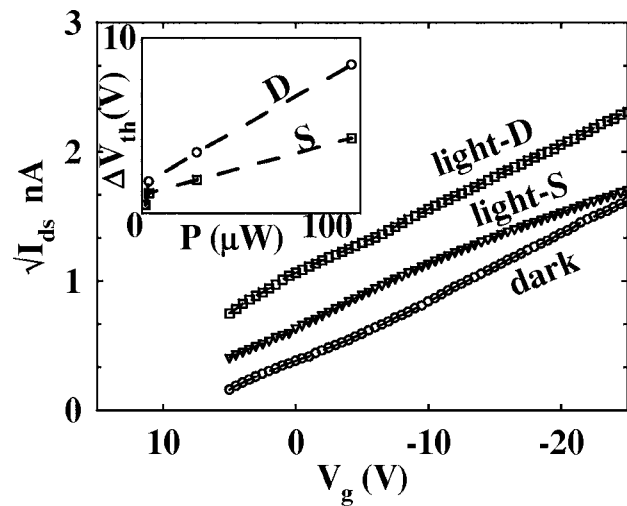


FIG. 2. $\sqrt{I_{ds}}(V_g)$ characteristics at $V_{ds} = -10$ V for P3HT FET in dark and with light ($120 \mu\text{W}$) incident selectively at the source and drain electrodes. The inset is the V_{th} shift with increasing incident intensity P .

The transconductance relation $I_{ds} = \{w/2L\}\mu C_i (V_g - V_{th})^2$ which incorporates the modified V_{th} appears to hold good for the range of measurements (note that μ and C_i do not vary with intensity). A clear linear shift in V_{th} as a function of incident power can be inferred from the Fig. 2 (inset). The device exhibits $\Delta V_{th} \sim 8.2$ V when illuminated with $P = 120 \mu\text{W}$ at the drain electrode region compared to $\Delta V_{th} \sim 3.1$ V at the source electrode for the same P . A linear dependence of the ΔV_{th} with increasing light intensity is observed with a slope of 0.03 V/ μ W for source illumination and slope of 0.06 V/ μ W for drain illumination [Fig. 2 (inset)]. The observation of larger changes in I_{ds} brought about by large enhancement V_g and/or large P is consistent with this simplistic treatment.

This behavior and trend in S and D illumination was verified by interchanging the S-D electrodes ($S \rightarrow D$, $D \rightarrow S$), to discount sample-electrode variations and other asymmetric inhomogeneities. These results and observations were confirmed by measurements on six independently fabricated devices. The effect was also present upon changing the gate electrode, and for a wide range gate-source overlap. These features were magnified for the P3HT-PCBM devices that have a higher degree of photoinduced charge separation and provides a larger photogenerated carrier density.¹⁵ The features for the P3HT-PCBM devices are $\Delta V_{th} \sim 19$ V and $\Delta V_{th} \sim 10$ V when illuminated ($P = 120 \mu\text{W}$) at the drain electrode and source electrode, respectively. The intensity dependence indicates a linear response of $\Delta V_{th}(P)$, with a slope of 0.02 V/ μ W for source illumination and 0.07 V/ μ W for drain illumination (Fig. 3). These trends in P3HT-PCBM devices point to processes which are more prominent but qualitatively analogous to the ones prevailing in P3HT devices.

The absence of V_{th} shift in dark for pristine P3HT and P3HT-PCBM devices as a function of V_d and the near-symmetric response upon interchanging the S-D polarity is indicative of an absence of the Schottky-type barrier at the metal-semiconductor interface. However, the $V_{th}(P)$ dependence and the difference in S-D response under illumination can be viewed in terms of a barrier which is accessible by photoexcitation. V_{th} in organic transistors has been analyzed in terms of two major contributions:¹⁶ $V_{th} = V_{fb} + V_{sc}$, where

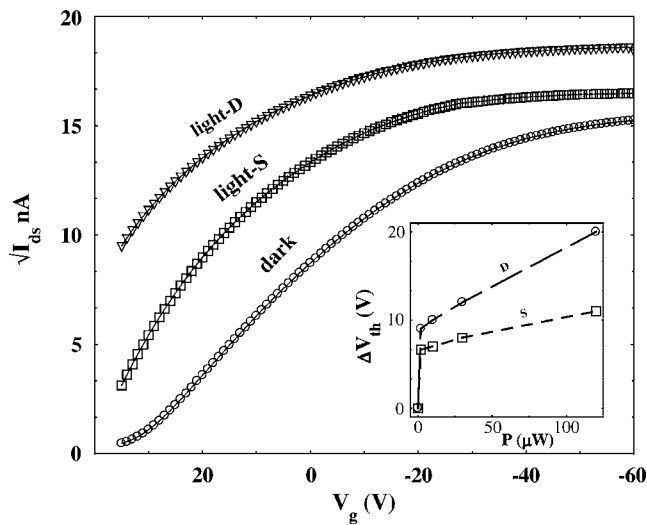


FIG. 3. $\sqrt{I_{ds}}(V_g)$ characteristics at $V_{ds} = -10$ V for P3HT-PCBM FET in dark and with light ($120 \mu\text{W}$) incident selectively at the source and drain electrodes. The inset is the V_T shift with increasing incident intensity P .

V_{sc} corresponds to voltage drop across the semiconductor and V_{fb} corresponds to flatband potential arising from any mismatch between work function of metal electrodes and semiconductor. The illumination and generation of charge carriers at a sufficient distance away from the channel region primarily affects V_{fb} but not V_{sc} . The flatband potential gets modified as the photogenerated carriers close to the metal-polymer interface enters the metal electrodes and shifts the band level so as to lower the barrier required for charge injection and collection. The results then can be interpreted in terms of an additional/higher resistance at the reverse biased source contact for a transport model consisting of $R = R_{bulk} + R_{source} + R_{drain}$. The asymmetric photogenerated carrier kinetics at S and D electrodes can lower R_{drain} compared to R_{source} . The observation is consistent with results obtained from scanning probe potentiometry where CR manifests itself as sizable potential drop at the S and D regions.^{17,18}

In summary, we observe subtle changes in the FET characteristics for light incident selectively on the electrodes. A distinct difference and trend is observed in the photoresponse when light perturbs the region beneath these electrodes. The results were interpreted in terms of a lower barrier for extraction compared to injection of charge carriers. The approach can be generalized and extended to probe other combination of metal-semiconductor interfaces to yield useful information.

We acknowledge Dr. Harish for useful discussions and the Department of Science and Technology for financial support

- ¹C. D. Dimitrakopoulos and P. R. L. Malenfant, *Adv. Mater. (Weinheim, Ger.)* **14**, 99 (2002).
- ²R. A. Street and A. Salleo, *Appl. Phys. Lett.* **81**, 2887 (2002).
- ³G. Horowitz, R. Hajlaoui, D. Ficuam, and A. El Kassmi, *J. Appl. Phys.* **85**, 3202 (1999).
- ⁴S. D. Wang, T. Minari, T. Miyadera, Y. Aoyagi, and K. Tsukagoshi, *Appl. Phys. Lett.* **92**, 063305 (2008).
- ⁵R. A. B. Devine, *J. Appl. Phys.* **100**, 034508 (2006).
- ⁶R. J. Kline, M. D. McGehee, and M. F. Toney, *Nat. Mater.* **5**, 222 (2006).
- ⁷V. E. Choong, M. G. Mason, C. W. Tang, and Y. Gao, *Appl. Phys. Lett.* **72**, 2689 (1998).
- ⁸V. I. Arkhipov, E. V. Emelianova, Y. H. Tak, and H. Bassler, *J. Appl. Phys.* **84**, 848 (1998).
- ⁹V. Necliudov, M. S. Shur, D. J. Gundlach, and T. N. Jackson, *Solid-State Electron.* **47**, 259 (2003).
- ¹⁰M. Shur, *Physics of Semiconductor Devices* (Prentice-Hall, New Delhi, 2002), p. 215.
- ¹¹R. J. Chesterfield, J. C. McKeen, C. R. Newman, C. D. Frisbie, P. C. Ewbank, K. R. Mann, and L. L. Miller, *J. Appl. Phys.* **95**, 6396 (2004).
- ¹²L. Burgi, H. Sirringhaus, and R. H. Friend, *Appl. Phys. Lett.* **80**, 2913 (2002).
- ¹³K. S. Narayan and N. Kumar, *Appl. Phys. Lett.* **79**, 1891 (2001).
- ¹⁴S. Dutta and K. S. Narayan, *Phys. Rev. B* **68**, 125208 (2003).
- ¹⁵N. S. Saricifti, L. Smilowitz, A. J. Heeger, and F. Wudl, *Science* **258**, 1474 (1992).
- ¹⁶G. Horowitz, R. Hajlaoui, H. Bouchriha, R. Bourguiga, and M. Hajlaoui, *Adv. Mater. (Weinheim, Ger.)* **10**, 923 (1998).
- ¹⁷K. Seshadri and C. D. Frisbie, *Appl. Phys. Lett.* **78**, 993 (2001).
- ¹⁸L. Burgi, T. J. Richards, R. H. Friend, and H. S. Sirringhaus, *J. Appl. Phys.* **94**, 6129 (2003).